

# Nature of Electron Scattering in $\text{LaAlO}_3/\text{SrTiO}_3$ Interfaces Near the Critical Thickness

C. J. Li, W. M. Lü,\* X. Renshaw Wang, X. P. Qiu, L. Sun, S. W. Zeng, Z. Q. Liu, Z. Huang, Y. L. Zhao, Ariando, and T. Venkatesan\*

High-mobility 2D electron gas (2DEG) at the interface between polar insulator  $\text{LaAlO}_3$  (LAO) and nonpolar insulator  $\text{SrTiO}_3$  (STO) initially reported by Ohtomo and Hwang<sup>[1]</sup> has attracted extensive research on its origin,<sup>[2–14]</sup> properties,<sup>[15–25]</sup> and potential applications.<sup>[26–33]</sup> The unique features of transparency and field tuning capability in polar/nonpolar oxide interfaces will enable multifunctional optoelectronic devices. In such devices, controlling the carrier concentration and mobility will be crucial for device design and performance. Experimental efforts have demonstrated control of the mobility of 2DEG in this system by strain effect,<sup>[34]</sup> conducting atomic force microscopy biasing,<sup>[29–32]</sup> solvent effect on the polar surface,<sup>[35,36]</sup> and LAO stoichiometry.<sup>[9,10]</sup> However, a careful study of nature of various scattering mechanisms (e.g., carrier–carrier scattering, strain and magnetic center induced scattering) and their relative competition in a single system is not established yet.

The 2DEG is characterized by a metal–insulator transition (MIT) with more than four orders of magnitude of conductance change in LAO/STO interface between 3 and 4 uc of the polar layer.<sup>[15]</sup> In the vicinity of the MIT, one should expect great sensitivity of carrier density and mobility on the overlayer thickness. In this paper, we focus on LAO/STO with LAO thickness between 3 and 4 uc to search for the exact critical thickness of the MIT and investigate further the transport properties (carrier density and mobility) with aid of electric field effect. Dramatic changes in the transport properties are seen over a small range of variation of the polar layer thickness about the critical value and we are able to sort out the effect of lattice strain, carrier–carrier and magnetic scattering effects on the mobility. These

results will enable us to design future oxide electronic devices with desired electronic properties.

LAO thin films with thickness between 3 and 4 uc were deposited on  $\text{TiO}_2$ -terminated (001) STO substrates at 750 °C and 1 mTorr oxygen pressure by pulsed laser deposition (KrF laser  $\lambda = 248$  nm) followed by post annealing at 600 °C at 0.5 bar oxygen flow for 1 h. The growth process was in situ monitored by reflection high-energy electron diffraction (RHEED) on the specular spot. The oscillation of RHEED intensity aided us to grow the exact overlayer thickness in a sub-uc regime. Surface morphology of deposited samples was measured by atomic force microscopy (AFM). The growth mode of LAO on top shows layer-by-layer growth mode, so the morphology of a fully covered unit cell will be very different from partially covered unit cell. **Figure 1a,b** show the morphology of 3 and 3.5 uc LAO/STO. The clean terrace pattern in 3 uc sample is very similar to that of as treated STO substrate, indicating high quality of epitaxial layer-by-layer growth of a fully covered LAO overlayer. On the contrary, the rough surface with islands on top of the terraces of the 3.5 uc LAO/STO shows the intermediate growth of one atomic layer. The average size of the islands is about 100 nm.

Essentially, 3.5 uc LAO on STO is 50% surface coverage of the fourth uc of LAO grown on STO. The control of the final morphology is by stopping the layer at a fraction of the growth period. This is a reasonable assumption since the deposition rate is held constant. For example, **Figure 1c,d** represent the RHEED intensity oscillation and the stopping at 3.6 and 3.8 uc of LAO growth, respectively. Since the period of the oscillation (i.e., rate of growth) is about 40 s, we can easily control the stopping point with the assistance of the oscillation pattern. This technique enables us to control the LAO overlayer thickness in a sub-uc scale and our resolution is 0.05 uc (deposition corresponding to two laser pulses).

**Figure 2a** shows the MIT at room temperature with LAO overlayer thickness increased by sub-uc step. The actual onset of transition occurred at 3.65 uc with five orders of magnitude of increase in conductance with 0.05 uc increment of LAO thickness from 3.6 uc of insulating sample. The value of 65% for critical coverage was measured for three samples with an accuracy of  $\pm 5\%$ . This subcritical thickness is higher than the previous study where Lee et al.<sup>[37]</sup> observed occasional 3.5 uc of LAO/STO showing an upturn of resistance at low temperature and with large variation of conductance among samples. In contrast, our 3.65 uc sample remains metallic down to 2 K which proves that the MIT we observed is sharper and more reproducible. As shown in **Figure 2b**, once the sample thickness is larger than 3.65 uc, it shows strongly correlated Fermi liquid behavior with  $\rho - \rho_0$  proportional to  $T^2$ , similar to 2DEG where LAO thickness is above 4 uc. We can hence conclude that the accurate critical thickness is  $65 \pm 5\%$  of the total area covered by the fourth unit cell of LAO.

C. J. Li, Dr. W. M. Lü, Dr. X. R. Wang, L. Sun,  
S. W. Zeng, Dr. Z. Q. Liu, Dr. Z. Huang, Dr. Y. L. Zhao,  
Prof. Ariando, Prof. T. Venkatesan  
NUSNNI-Nanocore  
National University of Singapore  
Singapore 117411, Singapore  
E-mail: elwlwm@nus.edu.sg; venky@nus.edu.sg



C. J. Li, Prof. T. Venkatesan  
National University of Singapore Graduate School for  
Integrative Sciences & Engineering (NGS)  
28 Medical Drive, Singapore 117456, Singapore  
Dr. X. R. Wang  
MESA+ Institute for Nanotechnology  
University of Twente  
P.O. Box 217, 7500 AE, Enschede, The Netherlands  
Dr. X. P. Qiu, Prof. T. Venkatesan  
Department of Electrical & Computer Engineering  
National University of Singapore  
Singapore 117576, Singapore

DOI: 10.1002/admi.201400437

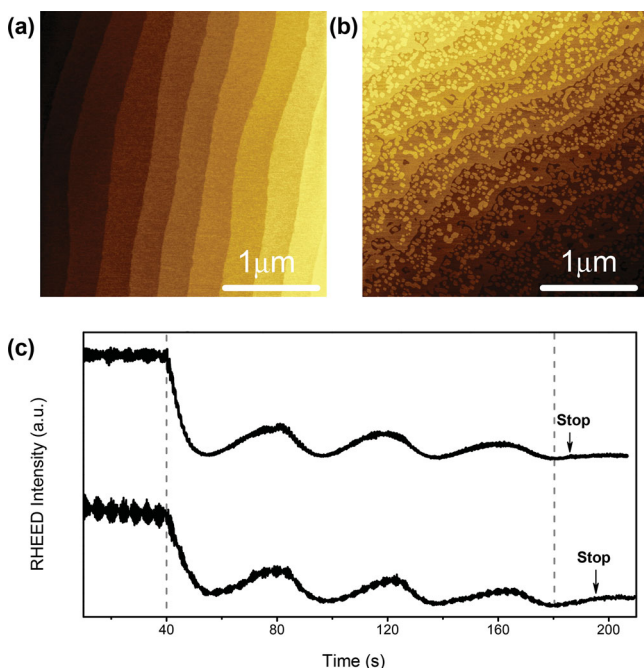


**Figure 1.** a,b)  $3 \times 3 \mu\text{m}^2$  AFM images of 3 and 3.5 uc LAO on  $\text{TiO}_2$ -terminated STO substrates, respectively. c) RHEED intensity oscillations of fractional layer growth of 3.6 and 3.8 uc of LAO, respectively. Dashed lines are guides to the eye.

The fourth polar layer critical thickness of 65% could be explained by 2D percolation theory. The fourth uc islands with size  $\approx 100$  nm shown in Figure 1b should be conducting.

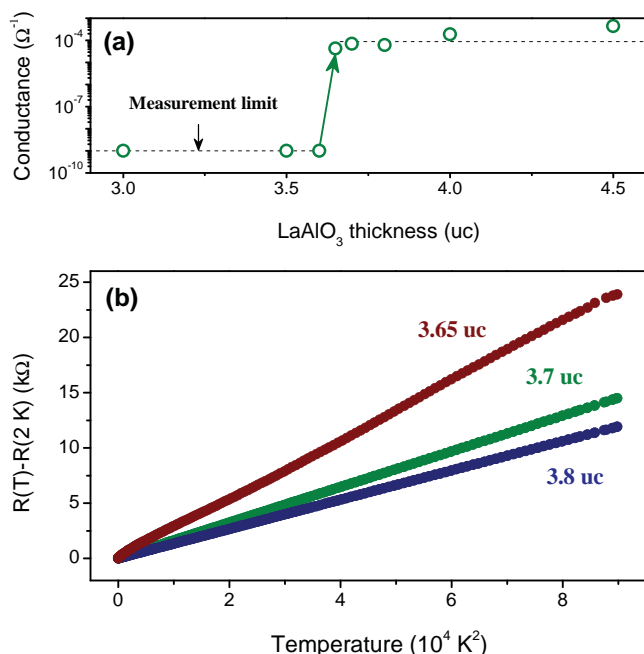


**Figure 2.** a) Room temperature (300 K) sheet conductance shows a sharp metal-insulator transition at LAO thickness of 3.65 uc. Dash lines are given as guides to the eye. b) Sheet resistance versus  $T^2$  of LAO/STO interface with different LAO layer thickness.

In order for global conductivity that can be measured across the  $5 \times 5 \text{ mm}^2$  area, the island density has to reach a critical value readily described by the 2D site percolation theory with a threshold between 0.593 (square-shaped islands) and 0.697 (honeycomb-shaped islands).<sup>[38]</sup> However, considering the dynamic deposition process of LAO growth where conducting islands nucleate and coalesce, it is not possible to define a single unique shape for the conductive islands (Figure 1b) leading to an average of 0.65 for the percolation threshold.

The 2DEG travels in the top few unit cells of STO.<sup>[19]</sup> The electron mobility will be affected by the lattice strain caused by the polar LAO layer (lattice mismatch of 3%), carrier-carrier scattering, and magnetic scattering if  $\text{Ti}^{3+}$  ions are created during the back biasing. Here we conducted a systematic study of these effects. Since carrier density saturates at 4 uc of LAO, we restricted our study to 3.5–4 uc of LAO with the carrier concentration varied by back gating of the STO. For reference, bare STO substrate carrier density was top gated by an ionic gel electrolyte in an electric double layer transistor configuration. **Figure 3a** shows the mobility dependence on the carrier density for LAO/STO interface with different LAO thicknesses at 2 K, the general

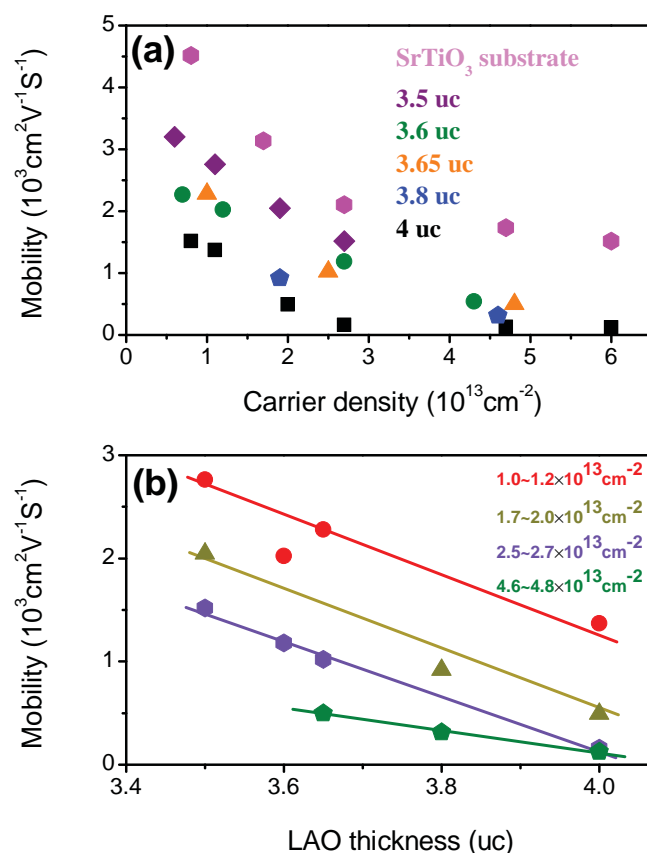


**Figure 3.** A wide range of carrier density of LAO/STO interface is achieved by field effect using STO as a back gate while variation of bare STO carrier density is achieved by top gating using ion liquid at 2 K. a) Carrier mobility versus carrier concentration of electrons (field induced and 2DEG of LAO/STO interface) with LAO thickness ranging from 3.5 to 4 uc b) Carrier mobility of 2DEG at LAO/STO interface versus LAO thickness for different carrier concentration ranges.

trend is lower mobility with increasing carrier density in the range of  $1 \times 10^{13}$ – $6 \times 10^{13}$  cm $^{-2}$ . This decreasing mobility with increasing carrier density is due to carrier–carrier scattering in the Fermi liquid. Mobility decreases linearly with increasing carrier density before saturation for 4 uc LAO/STO. The saturation trend is not observed in 3.5, 3.6, 3.65, and 3.8 uc samples most likely due to the maximum achieved carrier concentration are not high enough.

The other noticeable trend is that for similar carrier concentration, the thinner the overlayer, the larger the mobility, with the highest mobility observed in bare STO substrate. For example, with the carrier density level  $\approx 2.7 \times 10^{13}$  cm $^{-2}$ , the mobility of 3.5, 3.6, 3.65, and 4 uc samples are 1518, 1182, 1022, and 160 cm $^2$  V $^{-1}$  s $^{-1}$ , respectively. This trend is explicitly shown in Figure 3b where carrier mobility decreases linearly with the LAO thickness. In the carrier density range from  $1 \times 10^{13}$  to  $2.7 \times 10^{13}$  cm $^{-2}$ , the slope is a constant value of  $-2830$  cm $^2$  V $^{-1}$  s $^{-1}$  uc $^{-1}$ . The large slope shows extremely high sensitivity of carrier mobility on the surface coverage ratio of fourth unit cell of LAO, which has never been observed before. The effect of surface coverage on mobility is most likely due to the effect of strain, where the surface STO experiences a compressive strain by the coherent grown LAO layer on top. Since the 2DEG is confined at top few uc of STO,<sup>[19]</sup> which experience much larger strain from the LAO epitaxial layer than the bulk. Our trend of decreasing of mobility with increasing LAO thickness of the 2DEG at LAO/STO is consistent to previous report.<sup>[39]</sup> However, to date, such a high sensitivity of mobility on strain is only seen in the thickness interval between 3.5 and 4 uc of LAO across the MIT.

One interesting observation is that if we extrapolate the mobility versus LAO thickness curve to bare STO (0 uc LAO thickness) by the linear relationship obtained from 3.5 to 4 uc regime, the obtained mobility is much larger than that being measured from ionic liquid gating on STO for the same carrier concentration. This difference implies that there might be new scattering mechanisms introduced by the ionic liquid gating process, which was previously assumed to have no effect on the STO mobility. The effect on field-induced oxygen mobility at such interfaces has been pointed out by recent work.<sup>[40]</sup> The origin of additional scattering by ionic liquid STO interaction needs further study.

When the carrier density is high as  $4.7 \times 10^{13}$  cm $^{-2}$ , the slope is less steep with the value of  $-1060$  cm $^2$  V $^{-1}$  s $^{-1}$  uc $^{-1}$ , meaning weaker influence of LAO thickness. The lower sensitivity of mobility on surface coverage of LAO at higher carrier density ( $4.7 \times 10^{13}$  cm $^{-2}$ ) indicates the onset of additional scattering mechanism. Kondo-like effect is demonstrated in 4 uc LAO/STO and sub 4 uc LAO/STO through gating, very similar to

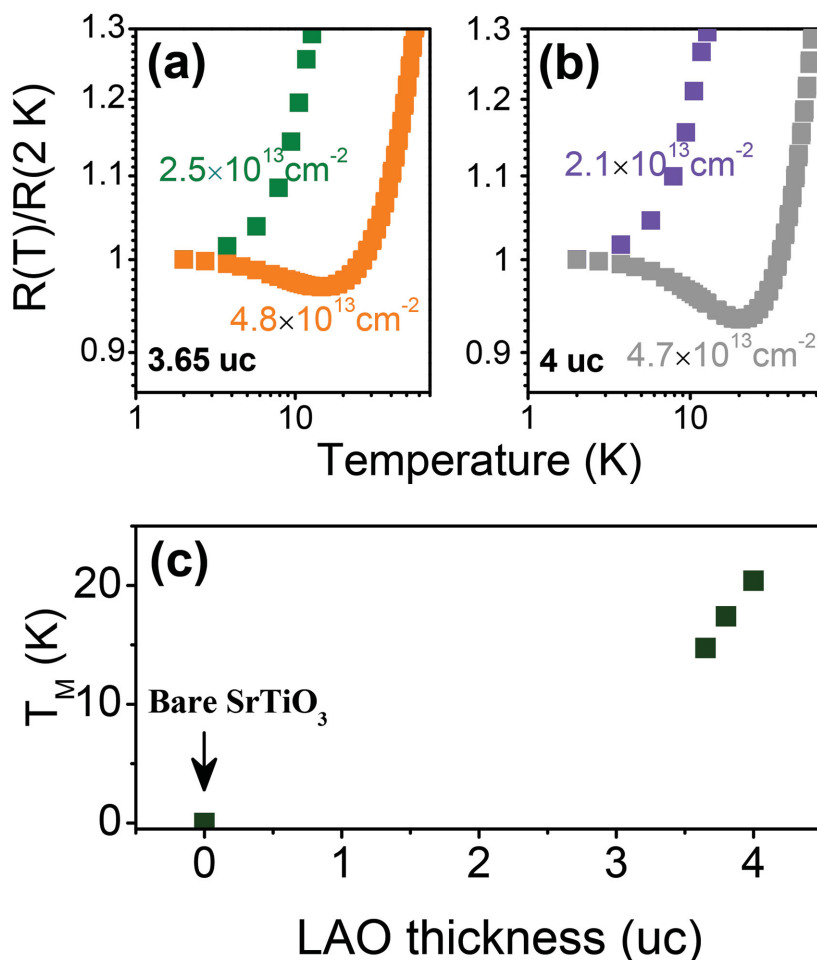


**Figure 4.** a,b) The sheet resistance versus temperature curves of LAO/STO for LAO thickness of 3.65 and 4 uc, respectively, for different carrier densities. c) LAO thickness dependence of the temperature of resistance minimum  $T_M$  at a carrier density of  $(4.5 \pm 0.3) \times 10^{13}$  cm $^{-2}$ .

what has been reported on bare STO substrate.<sup>[41]</sup> Figure 4a,b, respectively, show the induced Kondo-like resistance minimum for increasing carrier density by gating of 3.65 and 4 uc sample. The temperature of resistance minimum is also dependent on the overlayer thickness even though the carrier concentration is maintained at the same level. Figure 4c shows the temperature of resistance minimum when the carrier concentration is kept at  $4.8 \times 10^{13}$  cm $^{-2}$ . Top-gated STO substrate shows no upturn of resistance at low temperature while 3.65, 3.8, and 4 uc LAO/STO samples show temperature of resistance minimum at 15, 17, and 20 K, respectively.

Magnetoresistance (MR) is another way to confirm whether the resistance minimum is from Kondo effect. It is defined by  $MR(\%) = (R(B) - R(0))/R(0) \times 100\%$ , where  $R(0)$  is the resistance without magnetic field while  $R(B)$  is the resistance with magnetic field  $B$ . The sample position is defined by the angle  $\theta$  between magnetic field and the normal of sample surface. When  $\theta$  is  $0^\circ$  or  $180^\circ$ , field is out of plane and when  $\theta$  is  $90^\circ$ , magnetic field is in plane but perpendicular to current direction. As shown in Figure 5a, for a 3.65 uc sample, there is no resistance minimum when the carrier density is  $2.5 \times 10^{13}$  cm $^{-2}$ .

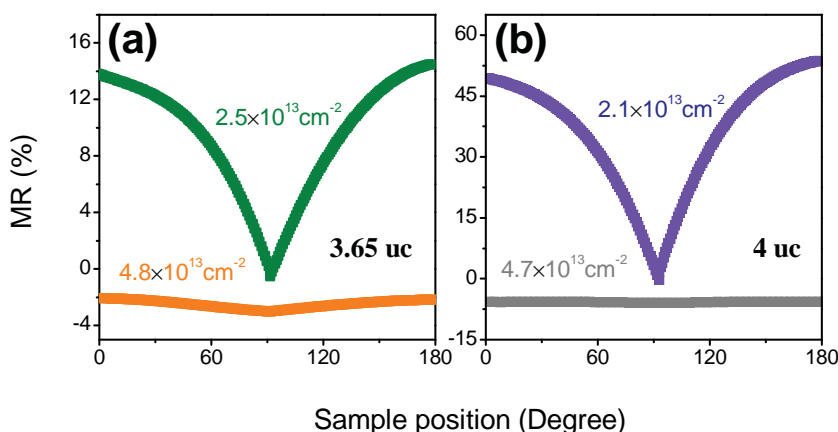


**Figure 5.** a,b) Angular dependent magnetoresistance of 3.65 and 4 uc LAO/STO, respectively, at different carrier densities at 2 K and a magnetic field of 2 T.

It shows anisotropic MR effect with positive MR up to 14% when the 2 T field is out of plane at 2 K, while for in plane field a tiny negative MR (less than -1%) is seen. This is similar to the typical 2DEG MR features with large anisotropy as reported before.<sup>[42,43]</sup> However, when the carrier density is tuned up to  $4.8 \times 10^{13} \text{ cm}^{-2}$  where it shows the resistance minimum at low temperature, MR becomes almost isotropic with a consistent negative value (-4%), which is one of the characteristic of Kondo scattering. For a 4 uc sample with carrier concentrations at  $2.1 \times 10^{13} \text{ cm}^{-2}$ , similar trend with stronger anisotropic MR (48% for out of plane MR and -2% for in plane MR) was observed at 2 T at 2 K; while at  $4.7 \times 10^{13} \text{ cm}^{-2}$ , isotropic negative MR as -6% was observed. The anisotropic MR observed at lower carrier density arises from orbital effects on scattering. Isotropic MR is more related to spin effect on scattering and that is why it is a characteristic of Kondo scattering. It also excludes the possibility of 2D weak localization that has an anisotropic MR signature.

The change from anisotropic to isotropic MR with only a factor of two increase of carrier density sheds light on the possible origins of the magnetic moments (necessary for Kondo scattering) at the LAO/STO interface. A similar trend in electrolyte-gated Kondo effect on  $\text{STO}^{40}$  was seen but at carrier concentration much higher ( $9.2 \times 10^{13} \text{ cm}^{-2}$  in bare STO vs  $4.7 \times 10^{13} \text{ cm}^{-2}$  in our 3.65–4 uc LAO/STO interface). The Kondo center is likely from localized  $\text{Ti}^{3+}$  with  $d^1$  electronic configuration. The  $\text{Ti}^{3+}$  state was confirmed by the electron energy-loss spectroscopy,<sup>[2]</sup> resonant inelastic X-ray scattering,<sup>[44]</sup> X-ray photoemission,<sup>[45,46]</sup> and X-ray absorption spectroscopy studies,<sup>[47]</sup> while electrolyte-gated bare STO single crystal was regarded as admixture of magnetic  $\text{Ti}^{3+}$  and delocalized electrons that fill the Ti 3d bands partially.<sup>[3,47,48]</sup> Our experimental results on the similarity among bare STO substrate and 3.5–4 uc thickness LAO/STO interfaces on tunable Kondo effect unifies the above two ideas. In short, electrons, either transferred from the LAO due to polar discontinuity or from electrostatic induction by back gating, can change the electronic states of Ti near the surface of STO leading to partially filled Ti 3d states. Part of them form localized magnetic centers  $\text{Ti}^{3+}$ , while the left over become delocalized and can be probed by transport measurements.<sup>[44,48]</sup>

The interaction between the two leads to the Kondo effect.

The differences between bare STO and LAO/STO interfaces are that LAO/STO interface needs much less carrier concentration to observe the similar Kondo effect. As described above, the compressive strain imposed by the LAO overlayer facilitates the localization of carriers and formation of localized magnetic moments, making the Kondo obvious even at a lower carrier concentration. This is also consistent with the fact that the temperature of resistance minimum is lower in thinner LAO/STO interface at the same concentration level (seen in Figure 4c). The experimental evidence on Kondo effect observed in 26 uc LAO/STO interface<sup>[17]</sup> with higher resistance minimum temperature

without external gating field also proves that strain tends to enhance Kondo scattering.

In conclusion, we observed a sharp critical thickness threshold for the onset of the 2DEG at the LAO/STO interface of  $3.65 \pm 0.05$  uc of LAO. The carrier–carrier scattering causes a linear carrier density dependent decrease of the mobility at low carrier concentration regime. Dramatic strain effects on the mobility are observed near the critical threshold. Enhancement of the carrier density by a factor of two using electric field effect leads to a significant onset of Kondo scattering most likely from  $\text{Ti}^{3+}$  ions at the interface. Furthermore, strain enhances the Kondo scattering at high carrier concentration. These experimental results will guide us in the fabrication of electronic and optoelectronic devices based on oxide interfaces.

## Experimental Section

**Sample Fabrication:** 3–4 uc LAO/STO samples were deposited by pulsed laser deposition technique. During the growth, the laser fluence was fixed at  $1.6 \text{ J cm}^{-2}$  and laser frequency was kept at 1 Hz. After growth, all samples were oxygen annealed at  $600^\circ\text{C}$  with 0.5 bar of oxygen flow for 1 h. Laser fluence, substrate target position and oxygen partial pressure and other experimental conditions were kept the same for all depositions to minimize the variation of LAO stoichiometry among samples. Prior to deposition, STO substrate was treated by buffered HF solution and annealed at  $950^\circ\text{C}$  in air for 2 h to get the  $\text{TiO}_2$  terminated STO.

**Transport Property Measurements:** Van der Pauw geometry electrical contacts were done by aluminum ultrasonic wire bonding on  $5 \times 5 \text{ mm}^2$  samples. Transport properties were carried in a physical property measurement system by Quantum Design with temperature range from 300 to 2 K. The measurements were done in a sealed chamber without light illumination in order to avoid possible photoconductivity effects.

The hall bar pattern on bare  $\text{TiO}_2$ -terminated STO substrate was defined by photolithography process with dimension of  $50$  (width)  $\times$   $160$  (length)  $\mu\text{m}^2$ . The electrodes of Ti (5 nm of thickness)/Au (100 nm of thickness) were deposited for the current and voltage leads. Ionic liquid for top gating is N,N-diethyl-N-methyl-N-(2-methoxyethyl)ammonium bis(trifluoromethyl sulphonyl)imide. A small drop of ionic liquid was spread between the gate electrode and the conducting channel and the gate voltage was applied up to 3.5 V.



## Supporting Information

Supporting Information is available from the Wiley Online Library or from the author.

## Acknowledgements

This work is supported by the Singapore National Research Foundation (NRF) under the Competitive Research Programs (CRP) "Tailoring Oxide Electronics by Atomic Control" (CRP Award No. NRF2008NRF-CRP002-024) and "New Approach To Low Power Information Storage: Electric-Field Controlled Magnetic Memories" (CRP Award No. NRF-CRP10-2012-02). X. R. W acknowledges financial support from the Dutch NWO foundation through a Rubicon grant (2011, 680-50-1114).

Received: September 25, 2014

Revised: October 29, 2014

Published online: November 19, 2014

- [1] A. Ohtomo, H. Y. Hwang, *Nature* **2004**, 427, 423.
- [2] N. Nakagawa, H. Y. Hwang, D. A. Muller, *Nat. Mater.* **2006**, 5, 204.
- [3] Z. S. Popović, S. Satpathy, R. M. Martin, *Phys. Rev. Lett.* **2008**, 101, 256801.
- [4] R. Pentcheva, W. E. Pickett, *Phys. Rev. Lett.* **2009**, 102, 107602.
- [5] P. R. Willmott, S. A. Pauli, R. Herger, C. M. Schlepütz, D. Martoccia, B. D. Patterson, B. Delley, R. Clarke, D. Kumah, C. Cionca, Y. Yacoby, *Phys. Rev. Lett.* **2007**, 99, 155502.
- [6] A. Kalabukhov, R. Gunnarsson, J. Börjesson, E. Olsson, T. Claeson, D. Winkler, *Phys. Rev. B* **2007**, 75, 121404.
- [7] W. Siemons, G. Koster, H. Yamamoto, W. A. Harrison, G. Lucovsky, T. H. Geballe, D. H. A. Blank, M. R. Beasley, *Phys. Rev. Lett.* **2007**, 98, 196802.
- [8] G. Herranz, M. Basletic, M. Bibes, C. Carrétéro, E. Tafr, E. Jacquet, K. Bouzehouane, C. Deranlot, A. Hamzić, J. M. Broto, A. Barthélémy, A. Fert, *Phys. Rev. Lett.* **2007**, 98, 216803.
- [9] M. P. Warusawithana, C. Richter, J. A. Mundy, P. Roy, J. Ludwig, S. Paetel, T. Heeg, A. A. Pawlicki, L. F. Kourkoutis, M. Zheng, M. Lee, B. Mulcahy, W. Zander, Y. Zhu, J. Schubert, J. N. Eckstein, D. A. Muller, C. S. Hellberg, J. Mannhart, D. G. Schlom, *Nat. Commun.* **2013**, 4, 2351.
- [10] E. Breckenfeld, N. Bronn, J. Karthik, A. R. Damodaran, S. Lee, N. Mason, L. W. Martin, *Phys. Rev. Lett.* **2013**, 110, 196804.
- [11] Z. Q. Liu, D. P. Leusink, X. Wang, W. M. Lü, K. Gopinadhan, A. Annadi, Y. L. Zhao, X. H. Huang, S. W. Zeng, Z. Huang, A. Srivastava, S. Dhar, T. Venkatesan, Ariando, *Phys. Rev. Lett.* **2011**, 107, 146802.
- [12] M. L. Reinle-Schmitt, C. Cancellieri, D. Li, D. Fontaine, M. Medarde, E. Pomjakushina, C. W. Schneider, S. Gariglio, P. Ghosez, J. M. Triscone, P. R. Willmott, *Nat. Commun.* **2012**, 3, 932.
- [13] Z. Q. Liu, Z. Huang, W. M. Lu, K. Gopinadhan, X. Wang, A. Annadi, T. Venkatesan, Ariando, *AIP Adv.* **2012**, 2, 012147.
- [14] Z. Q. Liu, C. J. Li, W. M. Lü, X. H. Huang, Z. Huang, S. W. Zeng, X. P. Qiu, L. S. Huang, A. Annadi, J. S. Chen, J. M. D. Coey, T. Venkatesan, Ariando, *Phys. Rev. X* **2013**, 3, 021010.
- [15] S. Thiel, G. Hammerl, A. Schmehl, C. W. Schneider, J. Mannhart, *Science* **2006**, 313, 1942.
- [16] A. D. Caviglia, S. Gariglio, N. Reyren, D. Jaccard, T. Schneider, M. Gabay, S. Thiel, G. Hammerl, J. Mannhart, J. M. Triscone, *Nature* **2008**, 456, 624.
- [17] A. Brinkman, M. Huijben, M. van Zalk, J. Huijben, U. Zeitler, J. C. Maan, W. G. van der Wiel, G. Rijnders, D. H. A. Blank, H. Hilgenkamp, *Nat. Mater.* **2007**, 6, 493.
- [18] N. Reyren, S. Thiel, A. D. Caviglia, L. F. Kourkoutis, G. Hammerl, C. Richter, C. W. Schneider, T. Kopp, A.-S. Rüetschi, D. Jaccard, M. Gabay, D. A. Muller, J.-M. Triscone, J. Mannhart, *Science* **2007**, 317, 1196.
- [19] M. Basletic, J. L. Maurice, C. Carretero, G. Herranz, O. Copie, M. Bibes, E. Jacquet, K. Bouzehouane, S. Fusil, A. Barthelemy, *Nat. Mater.* **2008**, 7, 621.
- [20] A. D. Caviglia, M. Gabay, S. Gariglio, N. Reyren, C. Cancellieri, J. M. Triscone, *Phys. Rev. Lett.* **2010**, 104, 126803.
- [21] Ariando, X. Wang, G. Baskaran, Z. Q. Liu, J. Huijben, J. B. Yi, A. Annadi, A. R. Barman, A. Rusydi, S. Dhar, Y. P. Feng, J. Ding, H.-U. Habermeier, T. Venkatesan, *Nat. Commun.* **2010**, 2, 188.
- [22] D. A. Dikin, M. Mehta, C. W. Bark, C. M. Folkman, C. B. Eom, V. Chandrasekhar, *Phys. Rev. Lett.* **2011**, 107, 056802.
- [23] L. Li, C. Richter, J. Mannhart, R. C. Ashoori, *Nat. Phys.* **2011**, 7, 762.
- [24] J. A. Bert, B. Kalisky, C. Bell, M. Kim, Y. Hikita, H. Y. Hwang, K. A. Moler, *Nat. Phys.* **2011**, 7, 767.
- [25] K. Michaeli, A. C. Potter, P. A. Lee, *Phys. Rev. Lett.* **2012**, 108, 117003.
- [26] C. W. Schneider, S. Thiel, G. Hammerl, C. Richter, J. Mannhart, *Appl. Phys. Lett.* **2006**, 89, 122101.
- [27] R. Jany, M. Breitschaft, G. Hammerl, A. Horsche, C. Richter, S. Paetel, J. Mannhart, N. Stucki, N. Reyren, S. Gariglio, P. Zubko, A. D. Caviglia, J. M. Triscone, *Appl. Phys. Lett.* **2010**, 96, 183504.
- [28] C. Cen, S. Thiel, G. Hammerl, C. W. Schneider, K. E. Andersen, C. S. Hellberg, J. Mannhart, J. Levy, *Nat. Mater.* **2008**, 7, 298.
- [29] C. Cen, S. Thiel, J. Mannhart, J. Levy, *Science* **2009**, 323, 1026.
- [30] G. Cheng, P. F. Siles, F. Bi, C. Cen, D. F. Bogorin, C. W. Bark, C. M. Folkman, J.-W. Park, C.-B. Eom, G. Medeiros-Ribeiro, J. Levy, *Nat. Nano* **2011**, 6, 343.
- [31] P. Irvin, Y. Ma, D. F. Bogorin, C. Cen, C. W. Bark, C. M. Folkman, C.-B. Eom, J. Levy, *Nat. Photon.* **2010**, 4, 849.
- [32] P. Irvin, J. P. Veazey, G. Cheng, S. Lu, C.-W. Bark, S. Ryu, C.-B. Eom, J. Levy, *Nano Lett.* **2013**, 13, 364.
- [33] J. W. Park, D. F. Bogorin, C. Cen, D. A. Felker, Y. Zhang, C. T. Nelson, C. W. Bark, C. M. Folkman, X. Q. Pan, M. S. Rzchowski, J. Levy, C. B. Eom, *Nat. Commun.* **2010**, 1, 94.
- [34] C. W. Bark, D. A. Felker, Y. Wang, Y. Zhang, H. W. Jang, C. M. Folkman, J. W. Park, S. H. Baek, H. Zhou, D. D. Fong, X. Q. Pan, E. Y. Tsybmal, M. S. Rzchowski, C. B. Eom, *Proc. Natl. Acad. Sci. USA* **2011**, 108, 4720.
- [35] Y. Xie, Y. Hikita, C. Bell, H. Y. Hwang, *Nat. Commun.* **2011**, 2, 494.
- [36] K. Au, D. F. Li, N. Y. Chan, J. Y. Dai, *Adv. Mater.* **2012**, 24, 2598.
- [37] J. S. Lee, S. K. Seung, S. R. Lee, J.-W. Chang, H. Noh, L. Baasandorj, H. S. Shin, S.-B. Shim, J. Song, J. Kim, *Phys. Status Solidi-Rapid Res. Lett.* **2012**, 6, 472.
- [38] D. Stauffer, A. Aharony, *Introduction to Percolation Theory*, Revised 2nd Edition Taylor and Francis London **1994**.
- [39] C. Bell, S. Harashima, Y. Hikita, H. Y. Hwang, *Appl. Phys. Lett.* **2009**, 94, 222111.
- [40] J. Jeong, N. Aetukuri, T. Graf, T. D. Schladt, M. G. Samant, S. S. P. Parkin, *Science* **2013**, 339, 1402.
- [41] M. Lee, J. R. Williams, S. Zhang, C. D. Frisbie, D. Goldhaber-Gordon, *Phys. Rev. Lett.* **2011**, 107, 256601.
- [42] M. Ben Shalom, C. W. Tai, Y. Lereah, M. Sachs, E. Levy, D. Rakhmilevitch, A. Palevski, Y. Dagan, *Phys. Rev. B* **2009**, 80, 140403.
- [43] X. Wang, W. M. Lü, A. Annadi, Z. Q. Liu, K. Gopinadhan, S. Dhar, T. Venkatesan, Ariando, *Phys. Rev. B* **2011**, 84, 075312.

- [44] K.-J. Zhou, M. Radovic, J. Schlappa, V. Strocov, R. Frison, J. Mesot, L. Patthey, T. Schmitt, *Phys. Rev. B* **2011**, *83*, 201402.
- [45] M. Sing, G. Berner, K. Goß, A. Müller, A. Ruff, A. Wetscherek, S. Thiel, J. Mannhart, S. A. Pauli, C. W. Schneider, P. R. Willmott, M. Gorgoi, F. Schäfers, R. Claessen, *Phys. Rev. Lett.* **2009**, *102*, 176805.
- [46] C. Cancellieri, M. L. Reinle-Schmitt, M. Kobayashi, V. N. Strocov, T. Schmitt, P. R. Willmott, S. Gariglio, J. M. Triscone, *Phys. Rev. Lett.* **2013**, *110*, 137601.
- [47] J. S. Lee, Y. W. Xie, H. K. Sato, C. Bell, Y. Hikita, H. Y. Hwang, C. C. Kao, *Nat. Mater.* **2013**, *12*, 703.
- [48] N. Pavlenko, T. Kopp, E. Y. Tsymbal, G. A. Sawatzky, J. Mannhart, *Phys. Rev. B* **2012**, *85*, 020407.
-